Effect of xanthan gum on the physical and mechanical properties of gelatin-carboxymethyl cellulose film blends

M.A.S.P. Nur Hazirah[a], M.I.N. Isa[b], N.M. Sarbon[a],*

[a] School of Food Science and Technology, Universiti Malaysia Terengganu, 21030 Kuala Terengganu, Terengganu, Malaysia
[b] School of Fundamental Science, Universiti Malaysia Terengganu, 21030 Kuala Terengganu, Terengganu, Malaysia

ABSTRACT

The aim of this study is to develop composite edible films from three different polymers to induce cross-link reactions that improved the quality of films made from two polymer types. Gelatin-carboxymethyl cellulose (CMC)-xanthan gum films were prepared by casting to study effects from the addition of different concentrations (0, 5, 10, 15, 20 and 25%, w/w solid) of xanthan gum to gelatin-CMC film. Physical and mechanical properties of the respective films were evaluated. The addition of xanthan gum increased the thickness, moisture content and water vapour permeability of gelatin-CMC film ($p < 0.05$). Furthermore, Ultraviolet (UV) light shielding increased along with reduced visible light transparency ($p < 0.05$) and increased thermal stability (T_g) ($p < 0.05$). No new functional groups formed although slight shifts in intensity values by Fourier Transform Infrared (FTIR) spectroscopy were observed. X-ray diffraction (XRD) analysis showed a diminished crystalline peak. The resulted films also demonstrated lower tensile strength with diminished elongation at the break point, as well as higher puncture force and lower puncture deformation, indicating higher puncture resistance than comparable gelatin-CMC film. Overall, gelatin-CMC film with xanthan gum (5%, w/w solid) demonstrated improved physical and mechanical properties more than films prepared from comparable formulations.

© 2016 Elsevier Ltd. All rights reserved.

1. Introduction

Food packaging is a crucial step in food manufacturing. Packaging contains and protects foods from physical damage and also from biological and chemical deterioration while providing multiple conveniences for consumers, including brand identity and contents. (Kim, Min, & Kim, 2014).

Presently, packaging films are used for perishable produce, meat and fish. Plastic films made from synthetic polymers have been increasingly used for food packaging due to their low price, easy moulding and superior mechanical and barrier properties (Jia, Fang, & Yao, 2009). However, they are non-degradable and non-renewable and cause serious environmental waste and pollution (Mu, Guo, Li, Lin, & Li, 2012). Consequently, biodegradable edible films have been developed as alternative packaging materials and are of great interest for many researchers. Edible films are made from polysaccharides such as cellulose derivatives, chitosan, starch and various vegetable and microbial gums; proteins such as gelatin, corn zein, wheat gluten and soy protein; and lipids such as waxes, fatty acids and resins (Bourtoom, 2008).

Protein derivatives are the most attractive biopolymers for edible film formulations because they provide high nutritional value, superior mechanical properties and exhibit the most impressive O_2 gas barrier (Ou, Kwok, & Kang, 2004). Gelatin, obtained by the controlled hydrolysis of insoluble fibrous collagen components of skin, bones and connective tissues generated as waste during animal slaughtering and processing (Guo, Ge, Li, Mu, & Li, 2014), is presently the most preferable protein derivative as the base material for formulating edible films. This is due to its natural abundance, biodegradability, low cost and excellent functional and filmogenic properties (Arvanitoyannis, 2002). Gelatin-based films are also thin, flexible and useful for several food packaging applications, including drug delivery (Boanini, Rubini, Panzavolta, & Bigi, 2010). However, gelatin-based films alone present several problems that limit food packaging applications because they are brittle, have poor water vapour resistance, poor thermal stability and absorb moisture (Bigi, Cojazzi, Panzavolta, Roveri, & Rubini, 2002). The addition of plasticizers such as glycerol and sorbitol has been shown to reduce brittleness but at the same time, increase water permeability (Sobral, Menegalli, Hubinger, & Roques, 2001).

Crosslinking techniques introduced in the preparation of films forms intermolecular bonds between polymer chains (Hager, Vallons, & Arendt, 2012) which enhances water resistance, cohesion, rigidity and mechanical strength (Tropini, Lens, Mulder, & Silvestre, 2004). The blending of one or more polymer types can enhance crosslinking. Studies have shown improved gelatin film properties by blending with carboxymethyl cellulose (CMC) (Wiwatwongwana & Pattana, 2010) or xanthan gum (Guo et al., 2014).

CMC is a water soluble cellulose derivative with anionic linear β-(1→4)-linked glycopyranose residue (Su, Huang, Yuan, Wang, & Li, 2010) produced by the partial substitution of 2, 3, and 6 cellulose hydroxyl groups by carboxymethyl groups (Tong, Xiao, & Lim, 2008). Researchers are highly motivated to produce edible films from CMC due to their ability to form a continuous matrix (Ghanbarzadeh & Almasi, 2011). In contrast to gelatin films, CMC-based films are also easily water soluble as it contains a hydrophobic polysaccharide backbone and many hydrophilic carboxyl groups (Su et al., 2010). CMC also improves protein film mechanical properties by increasing thermal stability and the elasticity modulus (Wiwatwongwana & Pattana, 2010) as shown by the blending of soy protein isolate films with CMC (Su et al., 2010).

Xanthan gum is a pentasaccharide. It is a heteropolysaccharide which consists of D-glucose, D-mannose and D-glucuronic acid units that is derived from bacteria and fungi (Sworn, 2000). It is produced by submerged aerobic fermentation of a pure *Xanthomonas campestris* culture after undergoing submerged aerobic fermentation (Guo et al., 2014). Xanthan gum's film forming properties comprise pseudo-plastic rheological behaviour in an aqueous environment that is amenable to film fabrication because it is readily dispersed in cold or hot water with very little effect on its viscosity from either temperature or pH (Baldwin, Hagenmaier, & Bai, 2012). Gelatin films blended with xanthan gum produce a very transparent film with excellent ultraviolet light resistance, low total soluble matter and moisture content, low water vapour permeability, improved mechanical properties and thermal stability (Guo et al., 2014).

Gelatin based film generally has good functional properties, however it has several problems that limit application as packaging materials as reported in several studies. It is brittle, has poor water vapour barrier, thermal stability and can absorb high moisture (Bigi et al., 2002). Besides, its mechanical strength is also lower than that of synthetic polymers film (Bourtoom, 2008). Addition of plasticizers like glycerol and sorbitol reduced the brittleness of films but they increased water permeability of the film (Sobral et al., 2001). In addition, crosslinking method that has been introduced to improve the functional properties of edible films still has some limitations was reported by several researchers

where; physical crosslinking is difficult to obtain the desired amount of crosslinking (Yao, Liu, Chang, Hsu, & Chen, 2004), chemical crosslinking can lead to toxicity problem that make the film produced is no longer edible (Cao, Fu, & He, 2007) and enzymatic crosslinking has limited availability and high production cost (Galietta, di Gioia, Guilbert, & Cuq, 1998). Therefore, other types of natural and biodegradable cross-linkers that are free from the problems mentioned above have to be used as the alternative. Xanthan gum was reported to be compatible cross-linker to be blended with various materials; it may dissolves directly in many highly acidic, alkaline, alcoholic systems containing different components. It is also compatible with commercially available thickeners such as sodium alginate, carboxymethyl cellulose (CMC) and starch (Sharma, Naresh, Dhuldhoya, Merchant, & Merchant, 2006). Hence, the present work used xanthan gum as a crosslinking agent to form a potentially new natural and biodegradable composite film as an alternative material for food packaging industry. Therefore, the objectives of this study were to formulate gelatin-CMC-xanthan gum blended films and determine the physical and mechanical properties at different concentrations of xanthan gum added.

2. Material and methods

2.1. Materials

Bovine skin gelatin (Type B, ~225 Bloom), carboxymethyl cellulose (CMC), xanthan gum and glycerol (plasticizer) were purchased from Sigma Aldrich (St. Louis, MO, USA).

2.2. Methods

2.2.1. Film preparation

The film forming solutions were prepared according to the method described by Jahit et al. (2016), with some modification. The gelatin solution was prepared by dissolving gelatin powder (80%, w/w solid) in distilled water at room temperature for 30 min followed by heating at 50 °C for 20 min under continuous stirring. The CMC solution was prepared by dissolving CMC powder (20%, w/w solid) in distilled water while stirring at 50 °C for 30 min. The xanthan gum solution was prepared by dissolving xanthan gum powder (5, 10, 15, 20 and 25%, w/w solid) in distilled water while stirring for 30 min at room temperature (Arismendi et al., 2013). The prepared three separate solutions were mixed and blended together with glycerol (30%, w/w solid). The blending mechanism was demonstrated in Table 1. The mixture was constantly stirred at 50 °C for 20 min for gelatinization. Approximately 25 ml of each film forming solution was cast on a Petri dish and oven dried at 45 °C for 48 h.

Table 1
Formulation of film forming solution of gelatin based film blended with CMC and xanthan gum (gelatin/CMC/xanthan gum).

Film formulations	Composition of film forming solution				
	Gelatin (g)	CMC (g)	Xanthan gum (g)	Glycerol (g)	Water (ml)
Ctrl-control (80/20/0)	3.2	0.8	–	1.2	100
A Xanthan gum 5% (80/20/5)	3.2	0.8	0.2	1.2	100
B Xanthan gum 10% (80/20/10)	3.2	0.8	0.4	1.2	100
C Xanthan gum 15% (80/20/15)	3.2	0.8	0.6	1.2	100
D Xanthan gum 20% (80/20/20)	3.2	0.8	0.8	1.2	100
E Xanthan gum 25% (80/20/25)	3.2	0.8	1.0	1.2	100

2.2.2. Film thickness measurements

Film thickness was measured by digital micrometer (Digimatic Micrometer 406-350, Mitutoyo Corp., Japan) to the nearest of 0.001 mm. Five measurements were taken for each film: one at the sample's centre and four more at varied perimeter sites. An average value was calculated.

2.2.3. Determination of moisture content

A standard oven-dry method was used to determine moisture content. Approximately 1 cm^2 of cut film was weighed (± 0.0001 g) and oven dried at 105 °C for 24 h and then re-weighed (± 0.0001 g). Moisture content (MC) was calculated as the percentage of dried weight loss as follows:

$$\text{Moisture Content} (\%) = \frac{w_1 - w_2}{w_1} \times 100 \tag{1}$$

where w_1 was initial weight (g) and w_2 was sample's dry weight. All final determinations were recorded as the mean of three measurements.

2.2.4. Light transmission and transparency

Ultraviolet (UV) and visible (vis) light barrier properties were measured using a UV–vis spectrophotometer (50 Probe, Cary®, USA). Filmstrips of 1 cm $\times$ 4 cm were cut and placed directly into a test cell. Transmittance at selected wavelengths (200–800 nm) were measured. An empty cell test was used as reference.

Film transparency was calculated as follows:

$$\text{Transparency} = -\log T/x \tag{2}$$

where T is transmission (%) at 600 nm and x is film thickness (mm) (Han & Floros, 1997). All determinations were recorded as the mean of three measurements.

2.2.5. Determination of water vapour permeability (WVP)

Water vapour permeability (WVP) was measured following ASTM method (). Filmstrips of 2.5 cm $\times$ 2.5 cm were mounted onto a clean dry plastic cup containing 10 g of silica desiccant. The surface area of the film covering the cup and the weight (± 0.0001 g) of each covered cup were measured. Each covered cup was stored in a desiccator with distilled water. The weight (± 0.0001 g) of the covered cup was measured daily for seven days. WVP was calculated as follows:

$$\text{WVP} (\text{g mm/m}^2 \text{dPa}) = \frac{w \times x}{A \times t \times (P_2 - P_1)} \tag{3}$$

where (w) is the weight gain of the cup (g); x is average film thickness (mm); (A) is the film surface area exposed to the permeant (m^2); (t) is the time of gain (d); and (P_1–P_2) is the difference between the partial atmospheric vapour pressure with silica desiccant and pure water (2800 Pa at 24 °C) (Pa). All final determinations were recorded as the mean of three measurements.

2.2.6. Thermal analysis by differential scanning calorimeter (DSC)

Thermal properties were determined by using a differential scanning calorimeter (DSC) (DSC, TA Q2000 Instrument, USA). Approximately 5 mg (± 0.001 mg) of film was cut into small pieces and sealed in an aluminium pan. Each sample was heated at 10 °C min^{-1} from 30 to 200 °C. An empty aluminium pan was used as reference. The glass transition temperature ($T_{g,}$ °C) was obtained from the thermogram. All determinations were recorded as the mean of three measurements.

2.2.7. Structural analysis by Fourier transform infrared (FTIR) spectrometer

The secondary structures of the prepared films via the attenuated total reflection (ATR) mode of the Fourier Transform Infrared (FTIR) spectrometer (Nicolet is10, Thermo Nicolet 380, USA), were examined. Filmstrips of approximately 1 cm^2 were placed on the sample holder of the Smart iTR ATR. FTIR spectra were recorded from 600 to 4000 cm^{-1} at a resolution of 4 cm^{-1} with a total of 32 scans.

2.2.8. X-Ray diffraction (XRD) analysis

X-ray patterns for each film formulation were analyzed by X-ray diffractometry with Cu K-α radiation ($\lambda = 1.54$ Å) at 30 kV and 15 mA (MiniFlex II, Rigaku, Japan). Film samples (2 cm^2) were placed on the sample holder and secured by tape. Each sample was scanned between $2\theta = 3$–60° at a scanning rate of 2°/min.

2.2.9. Tensile strength (TS) and elongation at break point (EAB)

Tensile strength (TS) and elongation at break point (EAB) were determined with a texture analyzer (TA XT Plus, Stable Micro Systems, UK). Filmstrips of 1 cm $\times$ 7 cm were affixed to a pair of grips on the AT/G probe. Initial grip separation and cross-head speed were set at 50 mm and 1 mm/s, respectively.

TS was calculated by dividing the maximum load (N) by the cross-sectional area (m^2) as follows:

$$\text{TS} (\text{MPa}) = \frac{P}{(b \times d)} \tag{4}$$

where P is maximum load (N); b is sample width (mm); and d is film thickness (mm).

The percentage of EAB was calculated as follows:

$$\text{EAB} (\%) = \frac{l_{\max}}{l_o} \times 100 \tag{5}$$

where $l_{\max}$ is film elongation (mm) at the moment of rupture; and l_o is the initial grip length (mm) of each sample. All final determinations were recorded as the mean of three measurements.

2.2.10. Puncture test

Puncture force and puncture deformation for each film sample were determined by the texture analyzer (TA XT Plus, Stable Micro Systems, UK) following the method described by Sobral et al. (2001), with modification. Each film sample was fixed to a 50 mm diameter annular space and perforated by a 3 mm diameter probe moving at 1 mm/s. Both puncture force (N) and probe displacement at breaking point (D) (mm) were determined. Puncture deformation (PD) was calculated as follows:

$$\text{PD} (\%) = \frac{\sqrt{D^2 + l_o^2} - l_o}{l_o} \times 100 \tag{6}$$

where l_o is considered the film's initial length, equal to the radius of the annular space (25 mm). All final determinations were recorded as the mean of three measurements.

2.3. Statistical analysis

Statistical analysis for a Completely Randomized Design (CRD) with Analysis of Variance (ANOVA) utilizing the Minitab 14.0 (Minitab Inc., State College, PA, USA) were undertaken. Comparison of means was performed by Fisher's Test with a confidence level of $p < 0.05$.

3. Results and discussion

3.1. Film thickness

Table 2 shows thickness measurement results for different formulations of gelatin-CMC-xanthan gum composite films in this study. Film thickness ranged from 0.09–0.14 mm. The films produced were sufficiently thin to qualify as film as defined by American Society for Testing and Materials (ASTM) (1985) (i.e. ≤0.25 mm), as well as by Embuscado and Huber (2009) (<0.3 mm).

Results showed significant difference ($p < 0.05$) between thickness values, although the volume for each film forming solution cast on each Petri dish was controlled during the casting process to ensure similar thickness values. These differences were likely due to the solid content of each film forming solution, which influences film thickness (Han & Krochta, 1999). The significant thickness increases were observed for gelatin-CMC ($p < 0.05$) films cast with increasing xanthan gum content, which appeared to have produced a more compact film network. As film thickness depends on film composition (Valenzuela, Abugoch, & Tapia, 2013), the observed thickness values increased as more component was added to the film. Due to its lowest solid content (two polymers: gelatin and CMC), the *control* sample had the lowest thickness value (0.09 mm) compared to formulations *A, B,C, D* and *E* (0.10, 0.12, 0.13, 0.13 and 0.14 mm), respectively; each of which comprised three polymers (gelatin, CMC and xanthan gum). Film *E* had the highest xanthan gum concentration (25%, w/w solid) and the highest thickness value (0.14 mm). These results suggested that xanthan gum formed a compact film network with gelatin and CMC molecules due to crosslinking within the film matrix, thus, resulting in increased thickness value. It appeared, therefore, that the highest concentration of xanthan gum developed the highest crosslinking effect within the film matrix, and thus, helped to form the most compact film network.

3.2. Moisture content

The moisture content value between gelatin-CMC film blend (*control*) with gelatin-CMC-xanthan gum film blend at 5–20% (w/w solid) xanthan gum added (formulations –*A* through –*D*), respectively presented a significance difference (p < 0.05) as shown in Table 2. Xanthan gum might interact with gelatin via hydrogen bonds that block hydroxyl positions capable of associating with water to reduce moisture content in gelatin films (Guo et al., 2014), whereas the same mechanism is also performed by CMC in gelatin-CMC film (Jahit, Nazmi, Isa, & Sarbon, 2016). Thus, adding xanthan gum increased the capability to form hydrogen bonds within the polymer matrix. The insignificant differences ($p > 0.05$) in moisture content between films *A* through *D* was likely due to similar capabilities in blocking the hydroxyl position of xanthan gum that may associate with water, at concentrations from 5 to 20% (w/w solid) therefore, resulting in

formation of hydrogen bond between xanthan gum and gelatin matrix.

However, the addition of xanthan gum at the highest concentration (25%, w/w solid) in Formulation *E*, significantly increased ($p < 0.05$) the film's moisture content. In gelatin-CMC-xanthan gum films, it appears that CMC and xanthan gum not only interacted with gelatin molecules, but also with each other. The latter interactions in formulation *E* could have led to a higher susceptibility to water with an increased affinity for binding water molecules due to the exposure of a larger number of hydroxyl groups present in both structures. This factor subsequently increased moisture content for the composite film as also reported by Martins et al. (2012) in their study, which blended κ-carrageenan to locust bean gum films for a specific formulation.

3.3. Light transmission and transparency

Table 3 shows light transmission and transparency values for each films. All formulations showed a decrease in light transmission with the increased concentration of xanthan gum added at 200 and 280 nm, respectively. Lower light transmission for the films indicated an excellent barrier for UV light which was in agreement with the study by Guo et al. (2014). The addition of xanthan gum significantly decreased ($p < 0.05$) light transmission wavelength at 200 and 280 nm, respectively. The increasing film thickness upon the increasing content of xanthan gum added in the film formulation penetrated the transmission of UV light through the film, so that the higher the concentration of xanthan gum added, the lower the UV light transmission. However, the addition of xanthan gum at concentrations up to 20% did not improve the UV light barrier property since no significant difference ($p > 0.05$) was observed between light transmissions for films *B* through *E* at both 200 and 280 nm, respectively. These results suggest that xanthan gum improves barrier properties of blended films against UV light by enhancing the prevention of UV transmission. For visible light transmission, as similar with the UV light transmission, the increasing film thickness upon the increasing content of xanthan gum in the film formulation lowered the transmission of visible light. No significant differences ($p > 0.05$) were noted between Films *D* and *E* at 350–800 nm, showing that both film formulations had similar degrees of visible light barrier properties. Lowered light transmission within visible ranges is most likely due to a higher light transmission barrier for higher concentrations of xanthan gum.

Transparency at 600 nm for the *control* film was recorded at 1.99, higher than the transparency index for bovine hide gelatin film (0.58) obtained by Ma et al. (2012). This suggests that gelatin-CMC films are less transparent than pure gelatin films. Increasing the concentration of xanthan gum in the blend from 5 to 25% (w/w solid) significantly elevated ($p < 0.05$) the transparency value, strongly suggesting that higher concentrations of xanthan gum decrease blended film transparency. Guo et al. (2014) found that

Table 2
Moisture content, water vapour permeability, tensile strength, elongation at break, puncture force and puncture deformation values for gelatin-CMC-xanthan gum film formulations.

Film formulations	Thickness (mm)	Moisture content (%)	Water vapour permeability (g mm/ m² d kPa)	Tensile strength (MPa)	Elongation at break (%)	Puncture force (N)	Puncture deformation (%)
Control	0.09 ± 0.001^c	21.97 ± 0.06^{ab}	24.40 ± 0.31^c	7.84 ± 0.30^a	91.35 ± 0.31^a	3.22 ± 0.06^c	68.41 ± 0.57^a
A	0.10 ± 0.011^{bc}	20.84 ± 0.34^b	27.56 ± 2.66^{bc}	4.88 ± 0.02^b	76.13 ± 0.95^b	4.24 ± 0.04^{ab}	60.85 ± 4.48^b
B	0.12 ± 0.009^b	21.37 ± 0.24^b	29.78 ± 0.41^b	2.68 ± 0.16^e	65.09 ± 0.52^c	4.68 ± 0.04^a	47.74 ± 3.06^c
C	0.13 ± 0.001^{ab}	20.60 ± 1.15^b	33.12 ± 1.12^{ab}	3.26 ± 0.15^{de}	51.66 ± 3.00^d	4.66 ± 0.04^a	38.99 ± 0.33^d
D	0.13 ± 0.002^{ab}	21.46 ± 0.38^b	33.94 ± 0.74^{ab}	3.41 ± 0.08^d	50.64 ± 1.24^d	3.85 ± 0.13^b	23.90 ± 2.11^e
E	0.14 ± 0.006^a	23.62 ± 0.31^a	36.38 ± 0.44^a	4.07 ± 0.33^c	62.35 ± 0.39^c	4.41 ± 0.30^{ab}	22.32 ± 0.35^e

Film formulations: *Control* (gelatin-CMC = G-CMC); *A* (G-CMC + xanthan gum 5% w/w solid); –*B* (G-CMC + XG 10%); *C* (G-CMC + XG 15%); *D* (G-CMC + XG 20%); *E* (G-CMC + XG 25%). Results expressed as means ± standard deviation. Mean values in the same column with different superscript letters ([a–b]) are significantly different ($p < 0.05$).

Table 3
Light transmission and transparency value of gelatin-CMC xanthan gum films at different formulation at selected wavelengths.

Film formulations	Light transmission at different wavelengths (%)								Transparency value at 600 nm
	200 nm	280 nm	350 nm	400 nm	500 nm	600 nm	700 nm	800 nm	
Control	0.09 ± 0.002^a	2.39 ± 0.326^a	31.91 ± 0.068^a	50.95 ± 0.899^a	59.22 ± 0.398^a	65.52 ± 1.676^a	68.26 ± 0.287^a	70.84 ± 0.241^a	1.99 ± 0.135^d
A	0.06 ± 0.002^b	0.88 ± 0.320^b	22.76 ± 1.749^b	34.23 ± 1.114^b	46.38 ± 0.447^b	51.82 ± 1.107^b	53.43 ± 0.068^b	54.81 ± 0.916^b	2.83 ± 0.388^c
B	0.04 ± 0.005^c	0.78 ± 0.432^b	12.38 ± 0.011^c	19.72 ± 1.705^c	26.09 ± 0.407^c	30.29 ± 1.824^c	32.02 ± 2.208^c	32.92 ± 2.221^c	4.50 ± 0.132^b
C	0.03 ± 0.005^{cd}	0.41 ± 0.008^b	9.10 ± 0.197^d	15.94 ± 1.150^d	18.64 ± 0.030^d	24.22 ± 1.187^d	26.11 ± 2.737^d	27.14 ± 3.126^d	4.89 ± 0.223^b
D	0.02 ± 0.004^d	0.11 ± 0.057^b	4.34 ± 0.168^e	8.34 ± 0.221^e	12.52 ± 0.170^e	15.58 ± 0.754^e	16.40 ± 0.488^e	17.58 ± 0.231^e	6.34 ± 0.270^a
E	0.02 ± 0.001^d	0.09 ± 0.012^b	3.42 ± 0.168^e	7.82 ± 0.009^e	11.56 ± 0.243^e	12.82 ± 0.878^e	15.13 ± 0.044^e	15.70 ± 0.270^e	6.50 ± 0.083^a

Film formulations: *Control* (Gelatin-CMC = G-CMC); *A* (G-CMC + xanthan gum 5% w/w solid); *B* (G-CMC + XG 10%); *C* (G-CMC + XG 15%); *D* (G-CMC + XG 20%); *E* (G-CMC + XG 25%). Results expressed as means ± standard deviation. Mean values in the same column with different superscript letters ([a–c]) are significantly different ($p < 0.05$).

crosslinking reactions caused a darker colouration of films in their study. Thus, an increase in the transparency value of gelatin-CMC-xanthan gum films might directly result from darker colours caused by crosslinking of xanthan gum with gelatin-CMC. This result also agrees with visual observation of the fabricated films, which appeared less transparent. There was no significant difference ($p > 0.05$) between films *B* (4.50) and *C* (4.89) or between films *D* (6.34) and *E* (6.50), with both sets showing similar degrees of transparency. This result is also supported by the film thickness, since the film with the increased thickness value showed the decreased transparency value.

3.4. Water vapour permeability (WVP) results

Table 2 shows water vapour permeability (WVP) values for the different formulations of fabricated gelatin-CMC-xanthan gum films observed in this study were significantly increased ($p < 0.05$) and graduated WVP values ($p < 0.05$) were observed after the addition of xanthan gum. The significant differences ($p < 0.05$) between WVP values obtained for the *control* and films *A, B, C, D* and *E* correspond with a study by de Carvalho and Grosso (2004) where crosslinking reactions influenced the moisture diffusion coefficient within the gelatin's network, indicating structural changes in the polymeric matrix after crosslinkers were introduced to gelatin films. Thus, in the present study, the addition of xanthan gum to gelatin-CMC film appears to have changed the structure of the polymeric matrix affecting the moisture diffusion coefficient within the gelatin-CMC network as influenced by crosslinking reactions within the composite films.

Films *C* and *D* were not significantly different ($p > 0.05$), thus indicating both of the formulations possessed similar degree of hydrophilicity. The addition of 25% (w/w solid) xanthan gum (film E) exhibited the maximum WVP value, revealing that the highest concentration of xanthan gum contributed to the highest degree of hydrophilicity of the film. Moreover, films comprising three components might have higher WVP values than those with only two components. The higher WVP results obtained for gelatin-CMC-xanthan gum films, compared to gelatin-CMC films, also agree with a study conducted by Tong et al. (2008), where pullulan-alginate-CMC films demonstrated higher WVPs than pullulan-CMC and pullulan-alginate films.

Results from the present study revealed that the addition of xanthan gum to gelatin-CMC films did not improve the water vapour barrier property but rather increased the film's water vapour permeability. Nevertheless, a reduced water vapour barrier allows movement of water vapour across the film, which can prevent condensation within the package that otherwise, serves to increase the microbial spoilage of packaged foods (Souza, Cerqueira, Teixera, & Vicente, 2010). Hence, such films may be suitable as primary packaging where (i) a water vapour barrier is not critical and where secondary protection can be provided by an outer wrap, or (ii) for the packaging of non-water-sensitive-food products (Tong et al., 2008).

3.5. Thermal analysis by differential scanning calorimeter (DSC)

A differential scanning calorimeter (DSC) is used in order to determine each fabricated film's thermal stability. The thermograms of each film formulation's single glass transition temperature (T_g) and single melting point (T_m) were obtained (Table 4). The T_g for *Control* film was 56.36 °C, which is higher than pure fish gelatin film T_g (29.8 °C; Hosseini, Rezaei, Zandi, & Ghavi, 2012), or plasticized bovine-hide gelatin film T_g (41 °C; Gómez-Estaca, Montero, Fernández-Martín, & Gómez-Guillén, 2009). This finding demonstrated greater thermal stability for gelatin-CMC film than for pure gelatin film. T_g values for CMC, pure CMC films and different plasticized CMC films were reported at ∼99, ∼75 and 69–71 °C, respectively, (Ghanbarzadeh & Almasi, 2011). The results obtained from this study showed that there was no significant difference ($p > 0.05$) from T_g control for the smallest concentration of xanthan gum (5%, w/w solid) in formulation *A* (Table 4). However, significant T_g value increases ($p < 0.05$) were observed for formulations with 10, 15 and 25% (w/w solid) xanthan gum components, respectively. Besides improving thermal stability, the addition of xanthan gum at three higher concentrations appears to have stimulated interactions and increased enmeshment between the film's three components (Guo et al., 2014). Furthermore, xanthan gum is a hetero-polysaccharide of ultra-high molecular weight (1–2 million) (Sharma et al., 2006), which means its addition to gelatin-CMC film increased the film's molecular weight and led to an increased T_g value. Thus, film *E*'s demonstration of the highest T_g value was likely due to its higher molecular weight.

In contrast to T_g results, insignificant differences ($p > 0.05$) between T_m values indicate that crosslinking reaction contributions from the addition of xanthan gum (all concentrations) did not affect T_m (Table 4). Crosslinking should increase the thermal stability of gelatin films by shifting T_m towards a higher value. The

Table 4
T_g values obtained from DSC thermograms for gelatin-CMC-xanthan gum film formulations.

Film formulations	T_g (°C)	T_m (°C)
Control	56.36 ± 0.55^b	138.76 ± 5.68^a
A	57.63 ± 0.38^b	154.53 ± 3.08^a
B	60.07 ± 0.38^{ab}	146.14 ± 14.98^a
C	60.48 ± 2.02^{ab}	137.98 ± 0.33^a
D	56.94 ± 0.67^b	138.68 ± 5.90^a
E	61.57 ± 0.38^a	134.09 ± 2.81^a

Film formulations: *Control* (gelatin-CMC = G-CMC); *A* (G-CMC + xanthan gum 5% w/w solid); *B* (G-CMC + XG 10%); *C* (G-CMC + XG 15%); *D* (G-CMC + XG 20%); *E* (G-CMC + XG 25%). Results expressed as means ± standard deviation. Mean values in the same column with different superscript letters ([a–b]) are significantly different ($p < 0.05$).

composite films produced for this study did demonstrate improved thermal stability as T_m values for all formulations were higher compared to bovine gelatin film T_m (65.06 °C) as reported by de Carvalho and Grosso (2004), and (66.2 °C) as reported by Ma et al. (2012). This finding was possibly due to the high T_m value attributed to melting crystalline CMC domains, since CMC films plasticized by glycerol showed T_m values between 153.5 and 170.7 °C (Ghanbarzadeh & Almasi, 2011). Another factor affecting T_m increase is that the hydroxyl groups of CMC and xanthan gum likely induce increased hydrogen bonds within the film's matrix.

3.6. Structural analysis by Fourier transform infrared (FTIR) spectrometry

Fig. 1 shows FTIR spectra for gelatin, CMC and xanthan gum powders while, Fig. 2, by comparison, shows the FTIR spectra for the different formulations of gelatin-CMC-xanthan gum blended films produced in this study. The spectrum for gelatin in Fig. 3 exhibited four amide bands representing vibrational modes of the peptide bond. Bovine gelatin exhibits bands at 3276.99 cm^{-1} corresponding with *amide A*; at 3077.08 cm^{-1} representing characteristic *amide B* NH stretching coupled with a hydrogen bond; 1628.89 cm^{-1} reflects the C=O stretching of *amide I* or hydrogen bonding coupled to COO; 1532.06 cm^{-1} indicates *amide II*'s bending vibrations from N—H groups and stretching vibrations of C—N groups; bands at 1202.91 cm^{-1} reflect vibrations from *amide III*'s plane of C—N and N—H groups of bound amide, or vibrations of glycine's CH$_2$ groups (Nur Hanani, Roos, & Kerry, 2014; Hashim et al., 2010).

The CMC spectrum showed transmission bands at 3262.61 cm^{-1} attributed to hydrogen bonding in the OH stretching region; bands at 2915.72 cm^{-1} represent C—H stretching associated with the methane ring of hydrogen atoms; bands at 1586.07 cm^{-1} indicate the presence of COO^{-} assigned to carboxyl group stretching; bands at 1413.42 cm^{-1} and 1323.15 cm^{-1} are assigned to OH stretching in-plane and symmetrical C—H

stretching; while bands at 1052 cm^{-1} and 1021.28 cm^{-1} might be characteristic of C—O stretching on CMC's polysaccharide skeleton (Chai & Isa, 2013).

The xanthan gum spectrum displayed transmission bands at 3281.36 cm^{-1} attributed to the axial deformation of the OH group; bands at 2903.36 cm^{-1} represent the axial deformation of CHO and C—H (perhaps due to the absorption of symmetrical and asymmetrical CH$_3$ or CH$_2$ stretching); bands around 1700–1800 cm^{-1} indicate axial deformation of C=O ester, carboxylic acid, aldehydes and ketones; bands at 1604.41 cm^{-1} can be assigned to the axial deformation of C=O from enols (-diketones); bands at 1405.19 cm^{-1} might characterize the deflection angle of C=H; and finally, bands at 1021.28 cm^{-1} could be characteristic of C—O axial deformation (Faria et al., 2011).

Comparing the FTIR spectrum of gelatin-CMC film (*control*) with spectra presented by gelatin-CMC-xanthan formulations, a slight shift in intensity attributed to functional groups was observed. This shifting of transmission bands likely resulted from functional group interactions between polymers in the composite films, which indicated excellent miscibility (Martins et al., 2012). The shifting of the *control's* transmission band from 3281.23 cm^{-1} to higher values at 3281.42, 3281.45, 3281.56, 3281.54 and 3281.49 cm^{-1} presented by films *A, B, C, D and E*, respectively, revealed robust interactions between the hydroxyl groups of CMC, xanthan gum and glycerol as they bonded with the gelatin's amino groups. These results corroborate similar findings on chitosan-cassava starch-gelatin films by Zhong and Xia (2008). Of note is that none of the composite films displayed gelatin's *amide-B* group since hydroxyl group interactions made it undetectable, which, in turn, broadened the intensity peak.

The most useful peak for infrared analysis of secondary structures in protein is the *amide-I* band between 1600 and 1700 cm^{-1} (Pranoto, Lee, & Park, 2007). The range of intensity values were detected by FTIR for all formulations was 1633.29–1633.47 cm^{-1}, indicating gelatin's β-sheet structure was present throughout (Hashim et al., 2010). The *control's* intensity value
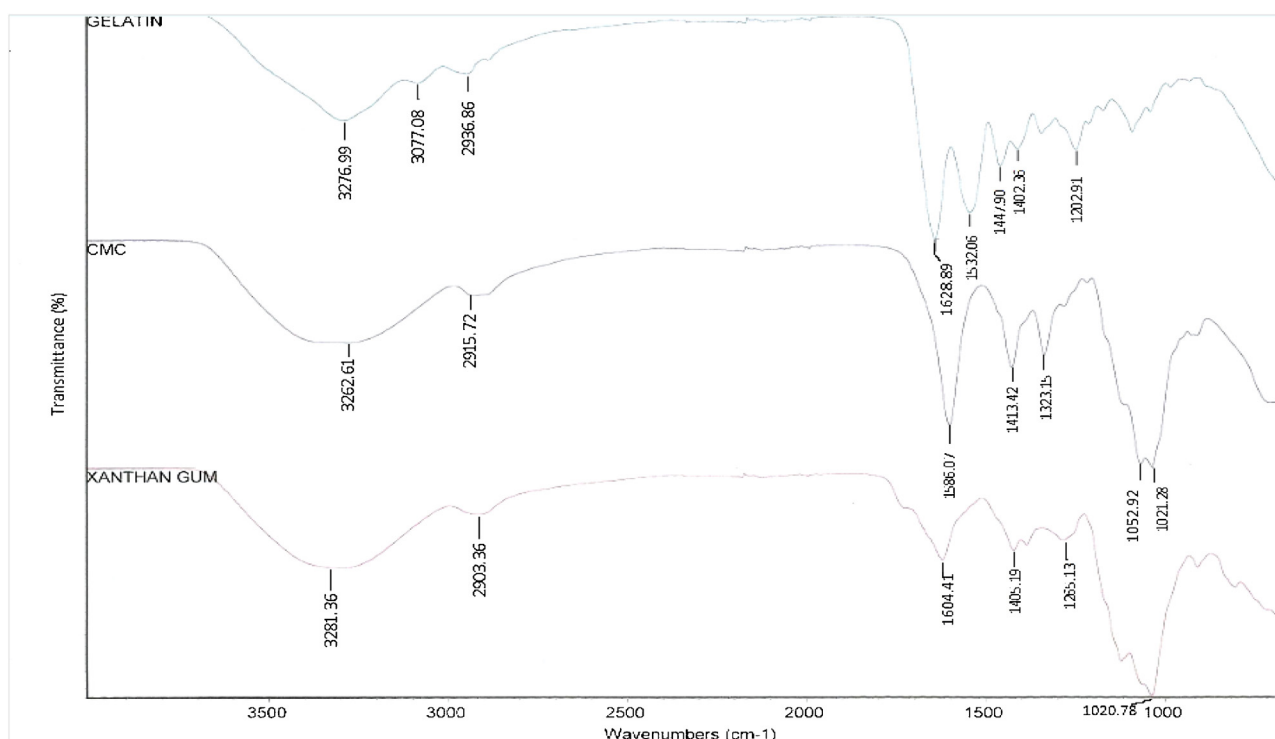

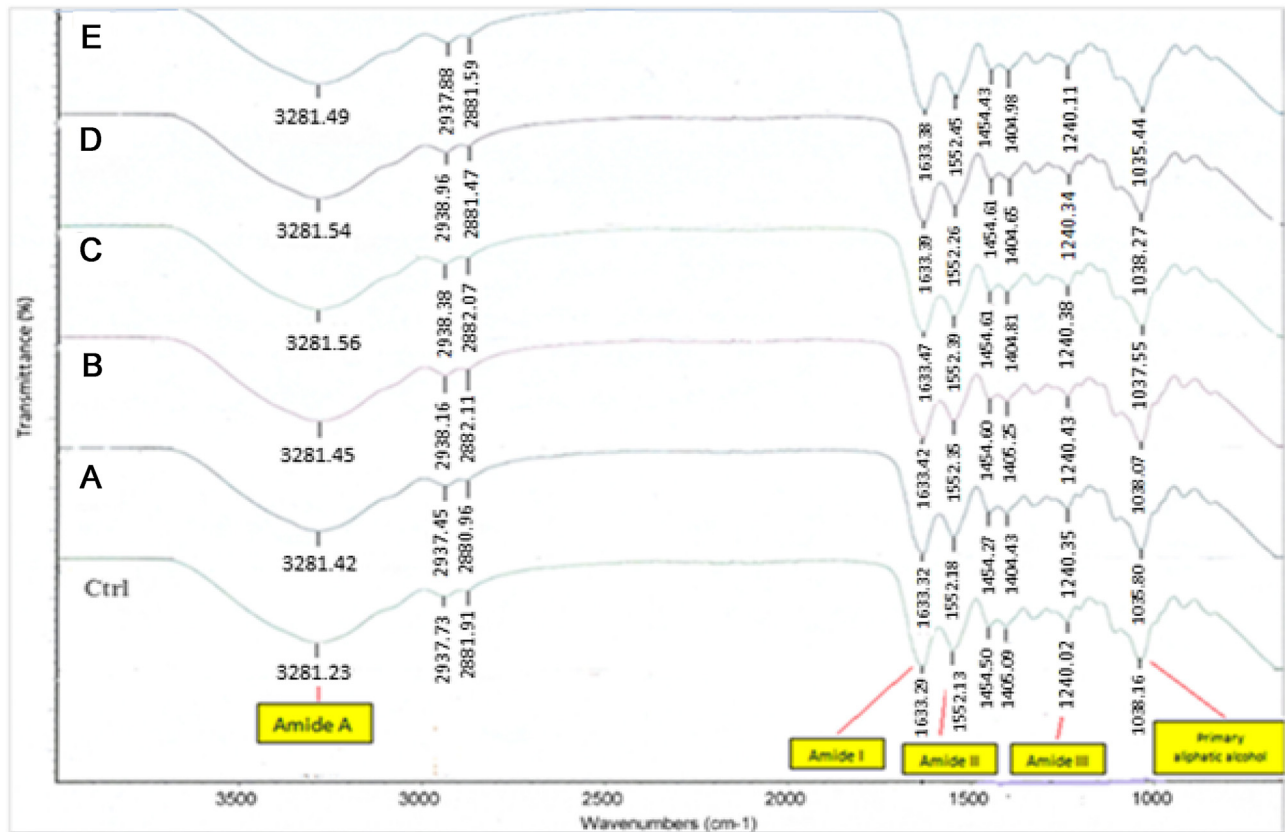**Fig. 1.** FTIR spectra of gelatin, CMC and xanthan gum films.

Fig. 2. FTIR spectrum of each gelatin-CMC-xanthan gum film formulation.
Film formulations: *Control* (gelatin-CMC = G-CMC); −*A* (G-CMC + xanthan gum 5% w/w solid); −*B* (G-CMC + XG 10%); −*C* (G-CMC + XG 15%); −*D* (G-CMC + XG 20%); −*E* (G-CMC + XG 25%).

shifted from 1633.29 cm^{-1} to 1633.32, 1633.42, 1633.47, 1633.39 and 1633.38 cm^{-1}, respectively, for each film (*A, B, C, D and E*). This indicated that interactions between the carboxylic groups of CMC and xanthan gum with *amide-I*, as well as crosslinking enhancement from the addition of xanthan gum, had strengthened the β-sheet structure of all composite films. *Amide-II* transmissions
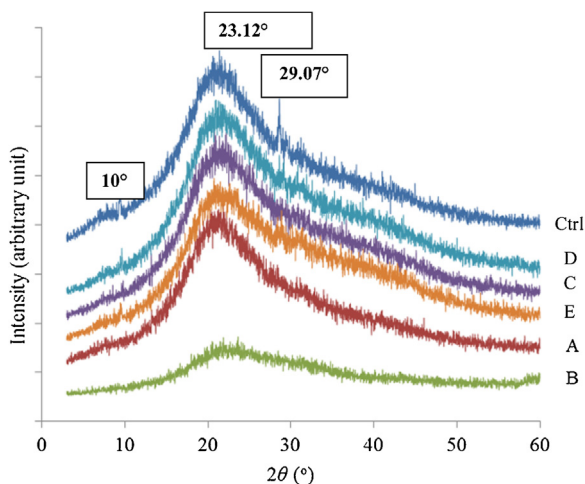

Fig. 3. XRD patterns of gelatin-CMC-xanthan gum film formulations demonstrating amorphous characteristics.
Film formulations: *Control* (gelatin-CMC = G-CMC); *A* (G-CMC + xanthan gum 5% w/w solid); *B* (G-CMC + XG 10%); *C* (G-CMC + XG 15%); *D* (G-CMC + XG 20%); *E* (G-CMC + XG 25%).

increased from 1552.13 cm^{-1} (*control*) to 1522.18, 1552.35, 1552.39, 1552.26 and 1552.45 cm^{-1}, respectively, for all composite films (*A, B, C, D and E*). *Amide-III* transmissions also increased from 1240.02 cm^{-1} (*control*) to 1240.35, 1240.43, 1240.38, 1240.34 and 1240.31 cm^{-1}, respectively, for all composite films (*A, B, C, D and E*). Furthermore, due to the polyelectrolyte characteristic of polymer chains in CMC and xanthan gum, electrostatic interactions related to amino and carbonyl moieties occurred in all films (Kocherbitov, Ulvenlund, Briggner, Kober, & Arnebrant, 2010; Hosseini et al., 2012). Hence, increased transmissions related to *amide-II* and *amide-III* suggest that the addition of xanthan gum to gelatin-CMC film strengthened electrostatic interactions between gelatin and CMC.

3.7. X-ray diffraction (XRD) analysis results

X-ray diffraction (XRD) patterns for all formulations (*control, A, B, C, D and E*) were obtained to assess film structure. Fig. 3 lists results obtained from 2θ intensity values of XRD patterns for each film formulation. The *control* film demonstrated a semi-crystalline structure with two major diffraction peaks: at 2θ = 23.12°, showing an amorphous peak, and at 2θ = 29.07°, showing a crystalline peak. A study conducted by Chai and Isa (2013) reported an amorphous peak at 2θ = 21.00° for CMC films. The present study added gelatin to CMC and obtained a slight shift (to 23.12°) from gelatin and CMC interactions. The particularly sharp peak observed at 29.07° was likely due to unorganized microcrystallite molecular residue from CMC's bulkier anionic side group activities, which disrupted crystalline lattice formation during film preparation. These results agreed with a similar report from Martins et al. (2012) on blended

films made of κ-carrageenan and locust bean gum. The addition of xanthan gum to gelatin-CMC films (A, B, C, D and E), appears to have reduced the *control's* crystalline peak ($2\theta = 29.07°$). These latter films individually displayed only one diffraction peak ($2\theta = 20.13°$, $23.12°$, $19.50°$, $21.00°$ and $20.81°$), respectively. Again, the results agreed with Zhong and Xia (2008) whose incorporation of xanthan gum suppressed the crystalline peak of gelatin-CMC film and formed a single amorphous peak when cassava starch was added to chitosan films.

Moreover, a slight shoulder at about $10°$ was observed at a peak for XRD pattern of the *control* film, which was also observed by Martins et al. (2012), indicating a slight separation phase of the film's components (gelatin and CMC). Hence, the addition of xanthan gum to formulations A through E appears to have decreased the intensity of this shoulder due to crosslinking, which likely reduced the phase separation observed in the gelatin-CMC *control*.

The amorphous structures demonstrated by A through E films were likely the result of structural contributions from the principle components (xanthan gum, CMC and gelatin). The amorphous property of xanthan gum was established by a broad diffraction peak at $2\theta = 23.12°$, probably the result of its double helix conformation (Guo et al., 2014). Furthermore, Kocherbitov et al. (2010) found xanthan gum in a glassy state (amorphous solid) at room temperature. A study by Chai and Isa (2013) established the amorphous nature of CMC. Additionally, these XRD results supported the higher WVP of gelatin-CMC-xanthan gum films as the amorphous configuration contributes to a permeable rather crystalline impermeable structure (Souza et al., 2010).

3.8. Mechanical properties of films

3.8.1. Tensile strength (TS) and elongation at break point (EAB)

The results obtained for tensile strength (TS) and elongation at break point (EAB) determinations for all film formulations is shown in Table 2. TS significantly decreased ($p < 0.05$) from *control* (7.84 MPa) to 4.88, 2.68, 3.26, 3.41 and 4.07 MPa, respectively for films A through E. The decrease appeared consistent with increasing xanthan gum levels, indicating a weakening of intermolecular forces. The presence of the OH group (water) in xanthan gum gave the highest intensity FTIR result and likely reduced the film's stiffness and resistance to elastic force, and thus, lowered tensile strength for the composites. This result corresponds with a study by Jia et al. (2009) which found that a reduction in TS occurred when konjac glucomannan-chitosan films were added to soy protein isolate, which weakened intermolecular forces between film components.

The addition of xanthan gum from 10% (w/w solid) up to 25% (w/w) solid which represented by formulations B-E significantly increased ($p < 0.05$) due to the high crosslinking reaction offered by the increasing concentration of xanthan gum. Xanthan gum is a heteropolysaccharide with a high molecular weight (1-2 million) (Sharma et al., 2006). Hence, the addition of xanthan gum to gelatin-CMC film increased the molecular weight of the film. Due to the molecular weight factor, the increment of TS value of Films B-E could not exceed TS value of Film A since the concentration of xanthan gum in formulation A was the lowest and xanthan gum at the higher concentration certainly provided higher molecular weight to the films with the higher difficulty to involve in the migration.

Similarly, as presented in Table 2, xanthan gum addition to gelatin-CMC film (*control*) significantly decreased ($p < 0.05$) the EAB value from 91.35% to 76.13, 65.09, 51.66, 50.66 and 62.35%, respectively, for films *A, B, C, D and E*. This decrease in EAB values is likely caused by gelatin cross-links with transglutaminase, formaldehyde or gloxal (de Carvalho & Grosso, 2004). The

increased thickness of films with xanthan gum addition influenced the elastic property of the films, which resulted in the decreasing of the elongation at the break point possessed by the films. In addition, there was no significant difference ($p > 0.05$) in EAB values between films C and D was noted, indicating that increasing xanthan gum concentration from 15 to 20% (w/w solid) give similar effect to EAB. However, formulation E (xanthan gum at 25%, w/w solid) significantly increased the EAB value ($p < 0.05$), likely due to a higher degree of crosslinking reactions.

Generally, increased TS precedes a decrease in EAB (Tong et al., 2008), but results obtained in this study showed decreased TS values preceding decreased EAB values, which echoed a study by Jia et al. (2009). However, a reduction of EAB for the two composite films did occur as expected due to the increasing development of crosslinking within these films' three components. This result closely associates with the amorphous properties of formulations A through E films demonstrated by XRD analyses, showing that mechanical properties of composite films with low degrees of crystallinity were not superior to the *control* film's semi-crystalline structure. This is especially so since organized structure in polymers with a high degree of crystallinity leads to higher-quality mechanical properties (Souza et al., 2010).

3.8.2. Puncture test

A higher puncture force and lower puncture deformation are desirable characteristics, as per the puncture test, indicating a film's higher resistance to puncture. Results of puncture tests for puncture force and puncture deformation of the composite films in this study are shown in Table 2. The addition of xanthan gum to gelatin-CMC film significantly increased ($p < 0.05$) puncture force from 3.22 N (*control*) to 4.24, 4.68, 4.66, 3.85 and 4.41 N, respectively, for films A through E. The addition of xanthan gum appears to have increased the reinforcement of the film's matrix via crosslinking reactions. In support of this view, Denavi et al. (2009) determined that crosslinking between film components caused a reinforcement of the matrix that increased the film's breaking force. Apart from that, the increased thickness of films with the addition of xanthan gum in the film formulations caused the films require larger force to be punctured. In the present work, composites B and C showed the highest reinforcement as they exhibited the highest puncture force.

By contrast, the addition of xanthan gum significantly decreased ($p < 0.05$) puncture deformation from 68.41% (*control*) to 60.85, 47.74, 38.99, 23.90 and 22.32%, respectively, for films A through E. Increasing concentrations of xanthan gum increased protein crosslinking, and thus, increased reinforcement of the film, which allowed for film distortion and a lower degree of post-puncture deformation. This observed reduction agreed with a study by Denavi et al. (2009). The films' thickness also influenced the percentage of deformation possessed by the films after being punctured, in which the increasing thickness of the films resulted in the increasing puncture deformation. No significant difference ($p > 0.05$) in puncture deformation values between films D and E were observed, which indicated that increasing xanthan gum concentration up to 25% had no significant (further) effect on puncture deformation. The addition of 20% (w/w solid) of xanthan gum was sufficient to optimize reduction of the film's puncture deformation.

The ranges for puncture force and deformation obtained correspond to values reported by Denavi et al. (2009): 2–8 N for puncture force, and 15–90% for puncture deformation. Since gelatin-CMC-xanthan gum formulations A through E showed both higher puncture force and lower puncture deformation values than the gelatin-CMC *control*, xanthan gum addition undoubtedly improved puncture resistance in the films under study.

4. Conclusion

The optimal formulation to produce gelatin-CMC-xanthan gum film has been determined based on the comparison on the desirable properties exhibited by all the formulations from the test conducted. Formulation A with 5% (w/w solid) xanthan gum was found to be the optimal formulation. The least amount of xanthan gum as an additive component in gelatin-CMC film offered more desirable properties among the other formulations, since it produced a film with lower moisture content, the highest barrier of UV light transmission, the most transparent characteristic, the lowest water vapour permeability, the highest tensile strength and elongation at break point and higher puncture force. The use of xanthan gum a non-gelling nature, as an alternative crosslinking agent in gelatin/CMC film blend have formed a compatible blend of composite film and improved several physical and mechanical properties of gelatin/CMC film blend alone. As compared to *control* film (gelatin-CMC film), Film A is thicker, but its thickness value is still in the range of the standard film thickness value and has lower moisture content, lower UV light transmission, similar glass transition and melting temperature, higher puncture force and lower puncture deformation. Therefore, by having these properties, we suggest that these composite films may be applicable as primary packaging material. However, Film A has higher water vapour permeability, lower tensile strength and lower elongation at break than *control*. Thus, it may require the protection of outer, secondary packaging.

References

American Society for Testing and Materials (ASTM) (1985). *Standard terminology relating to plastic. Designation D883-00. Annual book of ASTM standards*. Philadelphia: American Society for Testing Materials.

Arismendi, C., Chillo, S., Conte, A., Nobile, M. A. D., Flores, S., & Gerschenson, L. N. (2013). Optimization of physical properties of xanthan gum/tapioca starch edible matrices containing potassium sorbate and evaluation of its antimicrobial effectiveness. *LWT—Food Science and Technology*, *53*, 290–296.

Arvanitoyannis, I. S. (2002). Formation and properties of collagen and gelatin films and coatings. In A. Gennadios (Ed.), *Protein-based films and coatings* (pp. 275–304).Boca Raton: CRC Press.

Baldwin, E. A., Hagenmaier, R., & Bai, J. (2012). *Edible coatings and films to improve food quality*, 2nd ed. Boca Raton: CRC Press.

Bigi, A., Cojazzi, G., Panzavolta, S., Roveri, N., & Rubini, K. (2002). Stabilization of gelatin films by crosslinking with genipin. *Biomaterials*, *23*, 4827–4832.

Boanini, E., Rubini, K., Panzavolta, S., & Bigi, A. (2010). Chemico-physical characterization of gelatin films modified with oxidized alginate. *Acta Biomaterialia*, *6*, 383–388.

Bourtoom, T. (2008). Edible films and coatings: characteristics and properties. *International Food Research Journal*, *15*(3), 1–12.

Cao, N., Fu, Y., & He, J. (2007). Mechanical properties of gelatin films cross-linked, respectively, by ferulic acid and tannin acid. *Food Hydrocolloids*, *21*, 575–584.

Chai, M., & Isa, M. I. N. (2013). The oleic acid composition effect on the carboxymethyl cellulose based biopolymer electrolyte. *Journal of Crystallization Process of Technology*, *3*, 1–4.

de Carvalho, R. A., & Grosso, C. R. F. (2004). Characterization of gelatin based films modified with transglutaminase, glyoxal and formaldehyde. *Food Hydrocolloids*, *18*, 717–726.

Denavi, G. A., Pérez-Mateos, M., Añón, M. C., Montero, P., Mauri, A. N., & Gómez-Guillén, M. C. (2009). Structural and functional properties of soy protein isolate and cod gelatin blend films. *Food Hydrocolloids*, *23*, 2094–2101.

Embuscado, M., & Huber, K. C. (2009). *Edible film and coating applications*. New York: Springer Science+Business Media p. 430.

Faria, S., de Oliveira Petkowicz, C. L., de Morais, S. A. L., Terrones, M. G. H., de Resendea, M. M., de Franca, F. P., et al. (2011). Characterization of xanthan gum produced from sugar cane broth. *Carbohydrate Polymers*, *86*, 469–476.

Gómez-Estaca, J., Montero, P., Fernández-Martín, F., & Gómez-Guillén, M. C. (2009). Physico-chemical and film-forming properties of bovine-hide and tuna-skin gelatin: a comparative study. *Journal of Food Engineering*, *90*, 480–486.

Galietta, G., di Gioia, L., Guilbert, S., & Cuq, B. (1998). Mechanical and thermochemical properties of films based on whey proteins as affected by plasticizers and crosslinking agents. *Journal of Dairy Science*, *81*, 3123–3130.

Ghanbarzadeh, B., & Almasi, H. (2011). Physical properties of edible emulsified films based on carboxymethyl cellulose and oleic acid. *International Journal of Biological Macromolecules*, *48*, 44–49.

Guo, J., Ge, L., Li, X., Mu, C., & Li, D. (2014). Periodate oxidation of xanthan gum and its crosslinking effects on gelatin-based edible films. *Food Hydrocolloids*, *39*, 243–250.

Hager, A., Vallons, K. J. R., & Arendt, K. (2012). Influence of gallic acid and tannic acid on the mechanical and barrier properties of wheat gluten films. *Journal of Agricultural and Food Chemistry*, *60*, 6157–6163.

Han, J. H., & Floros, J. D. (1997). Casting antimicrobial packaging films and measuring their physical properties and antimicrobial activity. *The Journal of Plastic Film and Sheeting*, *13*, 287–298.

Han, J. H., & Krochta, J. M. (1999). Water vapour permeability and wetting properties of whey protein coating on paper. *American Society of Agricultural Engineers*, *42*, 1375–1382.

Hashim, D. M., Che Man, Y. B., Norakasha, R., Shuhaimi, M., Salmah, Y., & Syahariza, Z. A. (2010). Potential use of fourier transform infrared spectroscopy for differentiation of bovine and porcine gelatins. *Food Chemistry*, *118*, 856–860.

Hosseini, S. F., Rezaei, M., Zandi, M., & Ghavi, F. F. (2012). Preparation and functional properties of fish gelatin–chitosan edible blend edible films. *Food Chemistry*, *136*, 1490–1495.

Jahit, I. S., Nazmi, N. N. M., Isa, M. I. N., & Sarbon, N. M. (2016). Effect of drying temperature on the mechanical and physical properties of gelatin-based films blended with CMC and chitosan for food packaging? *International Food Research Journal*, *23*(3), 1068–1074.

Jia, D., Fang, Y., & Yao, K. (2009). Water vapour barrier and mechanical properties of konjac glucomannan-chitosan-soy protein isolate edible films. *Food and Bioproducts Processing*, *87*, 7–10.

Kim, Y. T., Min, B., & Kim, K. W. (2014). General characteristics of packaging materials for food system. In J. H. Han (Ed.), *Innovations in food packaging*USA: Academic Press 14 pp.

Kocherbitov, V., Ulvenlund, S., Briggner, L., Kober, M., & Arnebrant, T. (2010). Hydration of a natural polyelectrolyte xanthan gum: comparison with non-ionic carbohydrates. *Carbohydrate Polymers*, *82*, 284–290.

Ma, W., Tang, C., Yin, S., Yang, X., Wang, Q., Liu, F., et al. (2012). Characterization of gelatin-based edible films incorporated with olive oil. *Food Research International*, *49*, 572–579.

Martins, J. T., Cerqueira, M. A., Bourbon, A. I., Pinhero, A. C., Souza, B. W. S., & Vicente, A. A. (2012). Synergistic effects between κ-carrageenan and locust bean gum on physicochemical properties of edible films made thereof. *Food Hydrocolloids*, *29*, 280–289.

Mu, C., Guo, J., Li, X., Lin, W., & Li, D. (2012). Preparation and properties of dialdehyde carboxymethyl cellulose crosslinked gelatin edible films. *Food Hydrocolloids*, *27*, 22–29.

Nur Hanani, Z. A., Roos, Y. H., & Kerry, J. P. (2014). Use and application of gelatin as potential packaging materials for food products. *International Journal of Biological Macromolecules*, *71*, 94–102.

Ou, S., Kwok, K. C., & Kang, Y. (2004). Changes in in vitro digestibility and available lysine of soy protein isolate after formation of film. *Journal of Food Engineering*, *64*, 301–305.

Pranoto, Y., Lee, C. M., & Park, H. J. (2007). Characterization of fish gelatin films added with gellan and κ-carrageenan. *LWT—Food Science and Technology*, *40*, 766–774.

Sharma, B. R., Naresh, L., Dhuldhoya, N. C., Merchant, S. U., & Merchant, U. C. (2006). Xanthan gum—a boon to food industry. *Food Promotion Chronicle*, *1*(5), 27–30.

Sobral, P. J. A., Menegalli, F. C., Hubinger, M. D., & Roques, M. A. (2001). Mechanical: water vapour barrier and thermal properties of gelatin based edible films. *Food Hydrocolloids*, *15*, 423–432.

Souza, B. W. S., Cerqueira, M. A., Teixera, J. A., & Vicente, A. A. (2010). The use of electric fields for edible coatings and films development and production: a review. *Food Engineering Reviews*, *2*, 244–255.

Su, J., Huang, Z., Yuan, X., Wang, X., & Li, M. (2010). Structure and properties of carboxymethyl cellulose/soy protein isolate blend edible films crosslinked by Maillard reactions. *Carbohydrate Polymers*, *79*, 145–153.

Sworn, G. (2000). Xanthan gum, In G. O. Philips, & P. A. Williams (Eds.), *Handbook of hydrocolloids* (pp. 186–202).2nd ed. UK: Woodhead Publishing.

Tong, Q., Xiao, Q., & Lim, L. (2008). Preparation and properties of pullulan-alginate-carboxymethyl cellulose blend films. *Food Research International*, *4*, 1007–1014.

Tropini, V., Lens, J. P., Mulder, W. J., & Silvestre, F. (2004). Wheat gluten films crosslinked with 1-ethyl-3-(3-dimethylaminopropyl) carbodiamide and *n*-hydroxysuccinimide. *Industrial Crops and Products*, *20*, 281–289.

Valenzuela, C., Abugoch, L., & Tapia, C. (2013). Quinoa protein-chitosan-sunflower oil edible film: mechanical, barrier and structural properties. *LWT—Food Science and Technology*, *50*, 531–537.

Wiwatwongwana, F., & Pattana, S. (2010). Characterization on properties of modification gelatin films with carboxymethyl cellulose. *The first TSME conference on mechanical engineering* (pp. 1–8)..

Yao, C., Liu, B., Chang, C., Hsu, S., & Chen, Y. (2004). Preparation of networks of gelatin and genipin as degradable biomaterials. *Materials Chemistry and Physics*, *83*, 204–208.

Zhong, Q. P., & Xia, W. S. (2008). Physicochemical properties of edible and preservative films from chitosan/cassava starch/gelatin blend plasticized with glycerol. *Food Technology and Biotechnology*, *46*(3), 262–269.